

**Silver nanoparticle - poly (n-isopropylacrylamide) conjugate
preparation: biological and chemical characterization studies of
the conjugates**

Basil Baby¹ and Maya Devi S²

¹Research scholar, Research and Development Center, Bharathiar
University, Coimbatore-641046, E Mail :basilvattappillil@gmail.com

²Assistant Professor, Department of Chemistry, NSS College of Engineering,
Palakkad- 678008, Kerala, E mail: mayadevi968@gmail.com, Ph: 9447217701

Abstract

Conjugation of nanoparticles with organic compounds are performed to enhance the activity and to increase their stability. This property would aid in developing different life saving biomedical products. Based on this objective, silver nanoparticle - poly (N-isopropylacrylamide) conjugate was developed with the aim of investigating its wound healing ability and biocompatibility in the present study. Chemical characterization of developed silver nanoparticles was also studied using FESEM and UV spectroscopic analysis.

Keywords: Silver nanoparticles, poly (N-isopropylacrylamide), Organic ligand, Wound healing, Biocompatibility.

1.0 Introduction

Silver nanoparticles exhibit unique optical properties in the visible spectrum produced by local surface plasmon resonance – SPR (1). Coupling of nearest neighbour nanoparticles within self-assembled arrays further results in new properties so-called collective SPR (2), which induces a shift of the plasmonic peaks or creates hot spots that depend on the interparticle distance (3). Early efforts were focused on synthesis of monodisperse nanoparticles with controlled organic chain length (4). Organic ligands on a nanoparticle surface play an important role in preventing nanoparticles from aggregating, which essentially enables control of interparticle spacing (5). The interparticle distance of the resulting nanoparticles are ill-defined, which limits the ability to tune the SPR. More complicated chemistry is involved during synthesis, which often also results in poor quality control of the monodispersity of the functionalized nanoparticles (6). One way to accomplish this is to use organic ligands that respond to external environmental stimuli (e.g., thermal or pH changes), in order to functionalize the nanoparticle surface (through chemical bonding) so that the interparticle spacing of the resulting functionalized nanoparticles varies in response to external temperature or pH changes (7).

In the recent past, there have been sincere efforts to prepare Ag-NPs–polymer composite materials for applications in the biomedical field. In a work by Li and co-workers [8], polyaniline/silver nanocomposite has been synthesized via in situ chemical oxidation polymerization of aniline in silver salt by some chemical method using H_2O_2 as an external medium. In a significant work by Shameli et al. [9], the antibacterial characteristics of silver/poly(lactic acid) (Ag/PLA-NC) nanocomposite film were investigated. Silver nanoparticles (Ag-NPs) were synthesized into biodegradable PLA via chemical reduction in a diphasic solvent. Silver nitrate and sodium borohydride, respectively, were used as a silver precursor and reducing agent in the PLA, which acted as a polymer matrix and stabilizer. In an interesting work by Thomas et al. [10], silver nanoparticles were introduced into poly(acrylamide-co-N-vinyl-2-pyrrolidone) network using a unique strategy, called “Breathing-in–breathing-out” process, using water and acetone as a swelling and shrinking agent for hydrogels respectively [11].

Based on the concept of conjugating silver nanoparticles with an organic compound, we developed a simple and reliable method to synthesize poly (N-isopropyl acrylamide) (PNIPAM) derivative functionalized silver nanoparticle conjugates that are responsive and highly stable to external environmental changes. Thus the conjugate may be used in developing different wound healing materials that could be able to prevent the growth of infectious agents at wound site.

It has long been known that silver, in its ionic form (Ag^+), is an environment friendly antimicrobial that is commonly used against many species of bacteria [12]. However, recent investigations of silver in the form of silver nanoparticles (Ag-NPs) have also demonstrated a similar effect at lower concentrations than with the ionic form; effective concentrations have been reported in the literature [13]. The possible use of silver nanoparticles (Ag-NPs) as antibacterial agent has, therefore, been investigated as a means of arresting increasing bacterial resistance to conventional bactericides and antibiotics [14]. The proposed mode of action of Ag-NPs is that they attach to the phosphate and sulfur groups that are part of the phospholipids cell membrane or to the membrane protein and severely damage the cell and its major functions such as permeability, regulation of enzymatic signalling activity and cellular oxidation and respiratory processes. Ag-NPs can penetrate the bacterial cell and accumulate to toxic levels that may cause death of the organism [15].

The objective of developing silver nanoparticle with poly (N-isopropyl acrylamide) compound with the aim of investigating its wound healing ability and biocompatibility was studied in the present study. Chemical characterization of developed silver nanoparticles was also studied using FESEM and UV spectroscopic analysis.

2.0 Materials and methods

2.1 Preparation of Ag nanoparticles (Maribel et al., 2009)

For the preparation of silver nanoparticles two stabilizing agents, Sodium Dodecyl Sulphate (SDS) and Citrate of sodium were used. For the synthesis of silver nanoparticles, silver nitrate solution (1mM) and 8% (w/w) Sodium Dodecyl

Sulphate (SDS) were used as a metal salt precursor and a stabilizing agent, respectively. Hydrazine hydrate solution with a concentrate (2mM) and Citrate of sodium solution (1mM) were used as a reducing agent. Citrate of sodium was also used as stabilizing agent at room temperature. The transparent colourless solution was converted to the characteristic pale yellow and pale red colour, when citrate of sodium was used as stabilizing agent. The occurrence of colour was indicated the formation of silver nanoparticles. The silver nanoparticles were purified by centrifugation. To remove excess silver ions, the silver colloids were washed at least three times with deionized water.

2.2 Preparation of Np-PNIPAM Composites (Ruben and Wolfgang, 2007)

Aqueous mixtures of 1mM silver nitrate and PNIPAM at indicated molar ratios of PNIPAM/Ag were prepared and stirred at room temperature. After 5 min of stirring, NaBH_4 was added to achieve a 3:1 molar ratio of $\text{NaBH}_4/\text{Ag}^+$. The solution was stirred for 5 min to react and then immediately diluted with water to 4 times the volume to stop the reaction. The diluted solution was then heated to 40°C during centrifugation at 16 600 g for 15 min to sequentially precipitate Ag-PNIPAM and then the polymer. The Ag-PNIPAM nanoparticles were recovered by centrifugation at 10000 rpm for 10 min and then resuspended in water. This process was performed twice, followed by freeze drying to recuperate the nanocomposite in a powder form for storage at -20°C .

2.3 Chemical characterization of Ag nanoparticles

Field emission scanning electron microscopy (FESEM)

The size and morphology of the synthesized silver nanoparticles using field emission scanning electron microscopy (JSM-7500F, JEOL, Japan) was analyzed. A minute drop of nanoparticle powder was cast on to a carbon-coated copper grid and subsequently transferred to the microscope. The high-resolution images of silver nanoparticles were recorded and the morphology of AgNPs was further studied.

UV-Vis spectrophotometer studies

The UV-Vis spectrophotometer (Elico–BL 198) was used to measure the wavelength between 300 and 800 nm to monitor the formation of silver nanoparticles at regular intervals. Dilutions of samples were made if the sample was too concentrated. The UV-visible reading was recorded and then analyzed using the Origin Pro or Microsoft Excel analysis tool.

2.34 Biological characterization of Ag-NIPAM conjugates

Development of wound healing materials coated with Ag-NIPAM composite

The functional coating of wound healing mesh material using the developed Ag-NIPAM composite was done by a standard two dip-coating technique (Gollwitzer et al., 2003). The technique started with the preparation of stable slurry with 500 mg of Ag-NIPAM composites in the molten polyethylene glycol (1000 mg) in a glass vial. The mixture was heated at the range of 60°C–70°C in a water bath to obtain homogeneous slurry. The resulting slurry was homogenized in a magnetic stirrer for 5–10 minutes. The wound healing mesh disk was cut (10mm) using sterile devices and dip-coated twice with intermittent drying (suspension coating method).

The dip-coating procedure was carried out in sterile glass beakers on a shaker (120 rpm) for 30 min, with a drying period of about 15 minutes between the two coating procedures, followed by drying at room temperature. All the coating steps were carried out under strict aseptic conditions. After the coating procedure, the materials were stored at 4°C for up to 15 minutes. In order to increase the composite load and prevent excessive increase in material thickness, the coating process were repeated for replicates of each sample. Subsequently, in order to slow down the release rate of composite from PEG coating and mitigate the friction effect between material surfaces, a second coating layer was formed using PVA (poly vinyl alcohol). PVA was dissolved in DMSO to acquire a 10% (w/w) solution. PEG coated materials were submerged into PVA solution three times for 1 minute each. The coated materials were left to dry on a clean bench for 24–48 hours at room temperature to remove residual DMSO. The wound healing mesh coated with Ag-NIPAM composite was subjected to determine its wound healing ability and biocompatibility property.

Determining the wound healing ability of composite – Wound scratch assay

L₉₂₉ mouse fibroblast cells grown in 24 well plates at a density (1 X 10⁵ cells per ml) with ~80 % confluence was taken for the analysis. A small linear scratch was created in the confluent monolayer by gently scraping with sterile cell scrapper as per the method of Liang et al. (2007). After creating a scratch on L₉₂₉ mouse fibroblast cell lines, the cell migration, cell proliferation and wound closure was measured for the selected concentrate (100 µg) of Ag-NIPAM composite at different time periods (0th hour, 12th hour and 24th hour). Migration of cells between the scratch site and the distance traversed by cells migrating into the denuded area which emphasize the self-healing was observed using phase contrast microscope for each time period.

***In vitro* biocompatibility studies of Ag-NIPAM composite using standard MTT assay methods (Ebtessam Saad Al-Sheddi et al., 2014)**

Cytotoxicity assay is often used to evaluate the *in-vitro* cytotoxicity of polymeric components as it is a quick, effective method for testing mitochondrial impairment and correlates quite well with cell proliferation. It is based on the use of tetrazolium salt 3-[4,5-dimethylthiazolyl-2]-2,5-diphenyl tetrazolium bromide (MTT), which can be converted to an insoluble blue formazan product by mitochondrial enzymes in viable cells. L₉₂₉ fibroblast cell line is often used to evaluate cytotoxicity of Ag-NIPAM composite.

The fibroblast cell lines were cultivated in 12-well-microtitre plates to reach confluence growth. The composite sample was applied directly to the developed fibroblast monolayer. Before cell seeding, the plates were pre-wetted in 70 % aqueous ethanol solution for 48 h, rinsed twice with ultrapure (deionized) water. The specimens were then seeded with L₉₂₉ fibroblast cell line at 10,000 cells per well according to routine cell-culture methods. The plates were incubated at 37°C and 5 % CO₂ for fifteen days. The effect of composite on the biocompatibility of fibroblast was evaluated using the photometric MTT assay.

At each time point, samples were taken from the 24-well plates and transferred into new plates for the MTT study. The MTT solution was prepared by dissolving the powder in phosphate buffered saline at a concentration 1 mg/ml. After 1hr of incubation, the purple crystals were dissolved by adding sodium dodecylsulphate (SDS) in a 1:1 mixture of water and dimethyl formamide (DMF)

at a concentration of 20% w/v. After adding 1ml of MTT medium (0.0005mg/ml) to each well, the plates were incubated for 3h, rinsed and desorbed in 100 ul of 70 % isopropanol. After being agitated rapidly at 400 rpm /min for 40 min, the dyed medium was transferred to 96-well plate, and read at 550 nm. The biocompatibility or cell viability is expressed as a percentage of the control sample (100 %).

Evaluating the efficacy of developed wound healing materials coated with Ag-NIPAM composite against wound causing bacteria

An Ag-NIPAM composite coated mesh sample was subjected to evaluate its efficacy against the wound causing organisms. Standard Disc diffusion method was used to evaluate the activity. Briefly, Mueller-Hinton agar plates (Composition g/L: Acid hydrolysate of Casein: 17.5 g; Starch: 1.5 g, Sodium chloride: 5.0 g, Agar 17.0 g; Final pH - 7.0 ± 0.2) plates were prepared by pouring 15 ml of media into sterile Petri dishes. The plates were allowed to solidify for 5min and 0.1ml inoculum was swabbed uniformly and allowed to dry for 60 sec. Premeasured disc shaped (20 mm in diameter) Ag-NIPAM composite coated wound mesh were placed on the Mueller-Hinton agar plates plates (seeded with test bacterial inoculum). The disc was gently pressed to attach on the agar surface using sterile conditions. A plain mesh without composite was also kept in the plate as control. All the plates were incubated at 37 °C for 24 to 48 h. At the end of incubation, the zone of inhibition formed around each material was measured in millimeter. Experiments were carried out in triplicates and the activity was expressed in Standard deviation values using Statistical Package for Social Sciences (SPSS - 9 for Windows 7.0) software.

3.0 Results and discussion

The synthesis of AgNPs was performed with 0.01 M of silver nitrate solution with marine alga extract in Erlenmeyer flask in the ratio of 1:10, respectively, at the initial time point of the synthesis reaction, and 0.01 M of silver nitrate solution without marine alga extract was maintained as a control. The solution remains colorless and showed no color change even after 48 h upon heating as shown in Fig. 3a. The reduction of silver nitrate (AgNO_3) was visually confirmed by the change of color from yellowish-brown to reddish-brown after 30 min of reaction

as shown in Fig. 3b. The color of the marine alga extract became turbid after the addition of aqueous AgNO_3 solution signifying the initiation of the reaction. The intensity of brown color increased in direct proportion to the heating period of 24 h followed by 48 h as shown in Fig. 3c, d

3.1 Chemical characterization of Ag nanoparticles

Field emission scanning electron microscopy analysis

A field emission scanning electron microscope (FESEM) was employed to analyze the morphology structure, size, shape, and distribution of the nanoparticles formed. From Fig. 1, it is evident that the silver nanoparticles were coalesced to nano-clusters. When the reaction mixtures of the synthesis medium of silver nanoparticles were indirectly heated for 48h, most of the nanoparticles tend to be aggregated as shown in Fig.1. When silver nanoparticles aggregate, the metal particles become electronically coupled and this coupled system has a different surface plasmon resonance than the individual particles.

UV-Vis spectrophotometer studies

In order to confirm the formation of silver nanoparticles in the developed conjugate, UV-Vis absorption studies revealed a strong characteristic absorption peak around 405 nm for the silver nanoparticles due to the surface plasmon resonance effect (Fig. 2). However, the plain PNIPAM did not revealed any peaks indicating the absence of silver in the sample. Similar results have also been reported by Thomas et al (10) when poly (acrylamide-co-acrylic acid) hydrogel/silver nanocomposites demonstrated a sharp surface plasmon resonance peak at 406 nm.

3.2 Biological characterization of Ag-NIPAM conjugates

Determining the wound healing ability of composite – Wound scratch assay

In vitro wound healing assays have commonly been applied to measure cell migration, cell proliferation and wound closure in response to stimulation with specific agents. In this study, the Ag-NIPAM composite used for the cell adhesion

studies was determined for its ability to improve wound healing by acting directly on L₉₂₉ mouse fibroblast cells.

After creating a scratch on L₉₂₉ mouse fibroblast cell lines, the cell migration, cell proliferation and wound closure was measured for a known concentration (100 µg) of Ag-NIPAM composite at three different time periods (0th hour, 12th hour and 24th hour). Fig. 3 corresponding to self-wound healing ability of the developed Ag-NIPAM composite showed that, at 0th hour, no cell migration and proliferation was observed for the known concentrate (100 µg) including control (Distilled water). At 12th hour, positive cell migration and cell proliferation was observed when compared to the control sample. After 24 hours, more cell proliferation was evident and thus indicating the better wound healing ability of Ag-NIPAM composite.

In vitro scratch assay could be recorded as an appropriate and inexpensive method for the wound healing potential of herbal composite used in the present research. Similar *in vitro* wound scratch assay method was recorded from the literature survey. Srinivasa Rao Bolla et al. (2019) recently investigated the wound healing capacity of *Aristolochia saccata* leaf extract by using *In vitro* wound scratch assay, where proliferative and migratory capabilities of test compounds could be monitored through microscopy studies. L₉₂₉ fibroblast cell line was used for the assay. Scratch assay showed 34.05 %, 70.00 %, 93.52 % wound closure at 12 hrs, 24 hrs and 48 hrs of incubation respectively. These results were similar compared to positive control which showed 37.60 %, 56.41% and 99.05 % of wound closure. As there was similar wound healing abilities were noted for many antimicrobial compounds from the literature survey on L₉₂₉ mouse fibroblast cell lines, it was proved that the developed Ag-NIPAM composite could be used for the development of novel tissue engineered wound healing materials.

Biocompatibility of the developed organometallic conjugates – MTT assay

The biocompatibility test of any medical product / devices / wound dressing is essential to assure its safety to the patients. Biocompatibility of the device is normally investigated using analytical chemistry, *in-vitro* test, and animal models. Here, the biocompatibility of non-adhering wound mesh materials coated with Ag-NIPAM composite was evaluated by cytotoxicity assay (*in-vitro*

cell culture model). *In-vitro* methods of cytotoxicity can demonstrate the occurrence of changes within the cells, ranging from cell death to very subtle alterations of certain cellular functions. Non-adhering dressings are commonly used during granulation, tissue formation, and re-epithelialization. Dressings' effects were investigated by comprehensive *in vitro* approach- MTT assay measuring cell viability after direct contact. MTT assay is often used to evaluate the *in-vitro* cytotoxicity of polymeric components as it is a quick, effective method for testing mitochondrial impairment and correlates quite well with cell proliferation. It is based on the use of tetrazolium salt 3-[4,5-dimethylthiazolyl-2]-2,5-diphenyl tetrazolium bromide (MTT), which can be converted to an insoluble blue formazan product by mitochondrial enzymes in viable cells. L₉₂₉ fibroblast cell line is often used to evaluate cytotoxicity of wound dressing mesh as tissue engineered skin containing different types of cells like keratinocytes, melanocytes, and fibroblasts.

The fibroblast cell lines were cultivated in 12-well-microtitre plates to reach confluence growth. The dressing samples (1.0 cm × 1.0 cm) were applied directly to the developed fibroblast monolayer. The effect of the different non-adhering dressings on fibroblast viability was evaluated using the photometric MTT assay. The wound dressing coated with Ag-NIPAM composite exhibited no effect on cell viability, indicating that they did not alter viable cell count over the respective study period (24 hours) compared to the untreated control samples. The results were described below separately for each selected concentration of synergistic drugs + carrier with the support of table values and graphical representations attributing for cell cytotoxicity and cell viability. The cytotoxic effect on cell viability and cell morphology was also depicted for each concentration of Ag-NIPAM composite in Fig. 4.

The biocompatibility of the synergistic drug concentrations (5, 10, 15, 20, 25 µg/ml) were tested. During the analysis, no significant cytotoxicity was observed for the selected drug concentrations; the cytotoxicity was ranging between 5.2 % and 14.7 %. Interestingly, higher cell viability for the drug concentrations was evident (85.3 % to 99 %). The cytotoxicity (%) of the drug combinations were 14.7 % for 5 µg, 7.1 % for 10 µg, 6.5 % for 15µg, 5.2 % for 20

μg and 0% for 25 μg . The cell viability (%) for the drug combinations were found to be 85.3% for 5 μg , 92.9 % for 10 μg , 93.5% for 15 μg , 94.8 % for 20 μg and > 99 % for 25 μg (Table-2).

In Fig. 4, the wound dressing mesh coated with selected concentrations (5, 10, 15, 20 $\mu\text{g}/\text{ml}$) do not have much cytotoxic effect, as they show high cell viability in all extract concentrations. Further, there was no significant difference in the morphology of the L₉₂₉ fibroblast cells after 24 hours of cell culturing in the cell culture media (DMEM). Even after 24 hours not much significant difference occurred on cell morphology of fibroblast cells even though some notable differences in cell morphology and appearance of few vacuoles have been found in 10, 15, 20, 25 μg concentrates. The appearance of these vacuoles may be due to the fusion of multiple membranes of fibroblast cells.

The results revealed that the drug concentration did not inhibit the growth of cells; thus indicating the biocompatibility of the synergistic drug combinations for the development of tissue engineered wound dressing materials.

Evaluating the efficacy of developed wound healing materials coated with Ag-NIPAM composite against wound causing bacteria

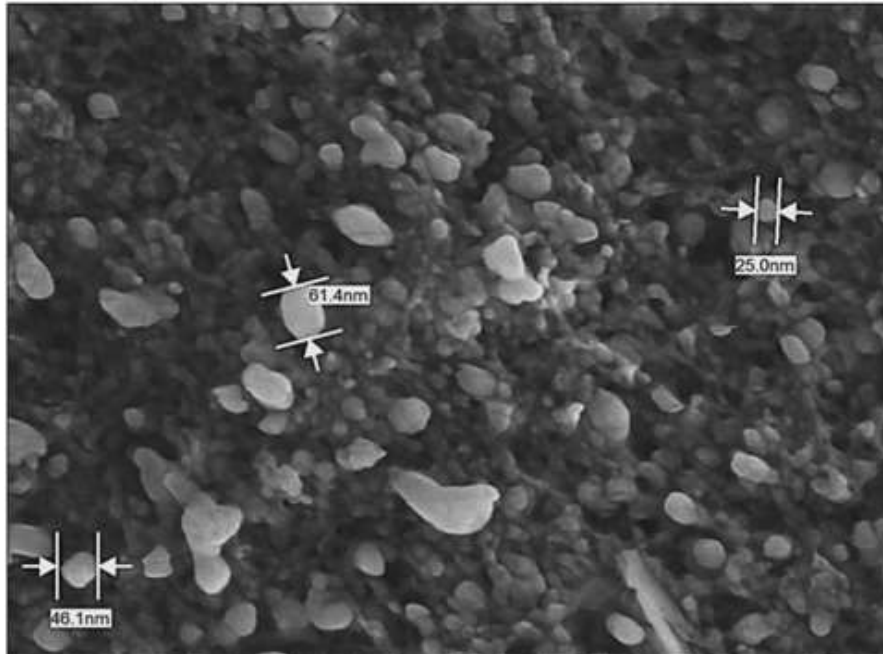
The efficacy of developed wound healing materials coated with Ag-NIPAM composite showed good inhibitory activity against wound causing bacteria. About 27.3 ± 0.56 mm and 27.1 ± 1.03 mm of inhibitory zone was observed for *Enterococcus faecium* and *Staphylococcus aureus*. Followed by, 27.8 ± 0.27 mm and 27.3 ± 0.56 mm of inhibitory zone was observed for *Klebsiella pneumonia* and *Acenitobacter baumannii*. *Proteus* sp. *Pseudomonas aeruginosa* exhibited 27.6 ± 1.03 mm and 27.9 ± 0.27 mm respectively (Table-1, Fig-5). The mechanism of action of the antibacterial activity of AgNPs is attacking the respiratory chain and cell division that ultimately leads to cell death. The silver nanoparticles have also been reported to release silver ions inside the bacterial cells, further enhancing their bactericidal activity (16). It has also been proposed that there can be release of silver ions by the nanoparticles, and these ions can interact with the thiol groups of many vital enzymes and inactivate them. The bacterial cells in contact with silver take in silver ions, which inhibit several functions in the cell and damage the cells. Then, there is the generation of reactive

oxygen species, which are produced possibly through the inhibition of a respiratory enzyme by silver ions and attack the cell itself. Silver is a soft acid, and there is a natural tendency of an acid to react with a base, in this case, a soft acid to react with a soft base (17).

Conflict of Interest

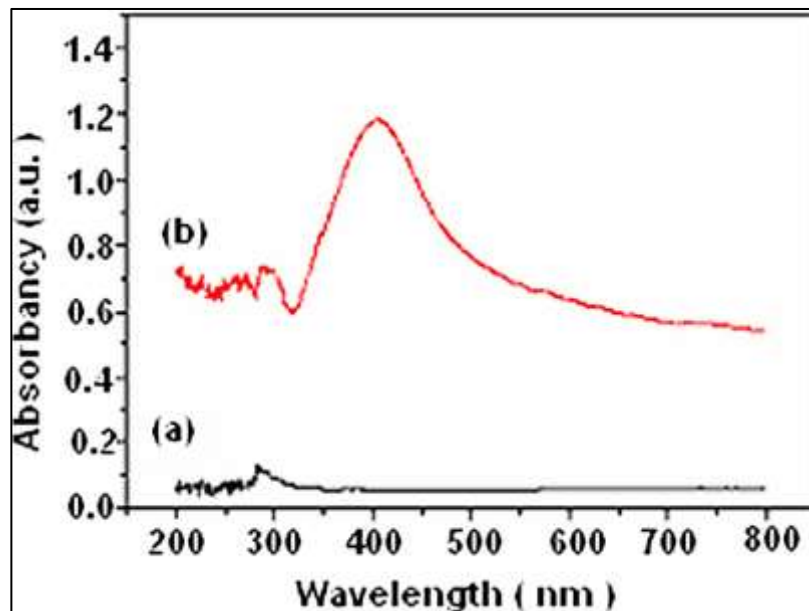
Authors declare no conflict of interest in the present research.

Fig-1: Field emission scanning electron microscopy analysis of silver nanoparticles



Coalesced nano-clusters of silver nanoparticles with varied size observed during FESEM analysis

Fig-2: UV-Vis spectrophotometer studies



(a) UV-Vis spectrophotometer studies of Silver nanoparticles in conjugate

(b) UV-Vis spectrophotometer studies of plain PNIPAM without silver nanoparticles

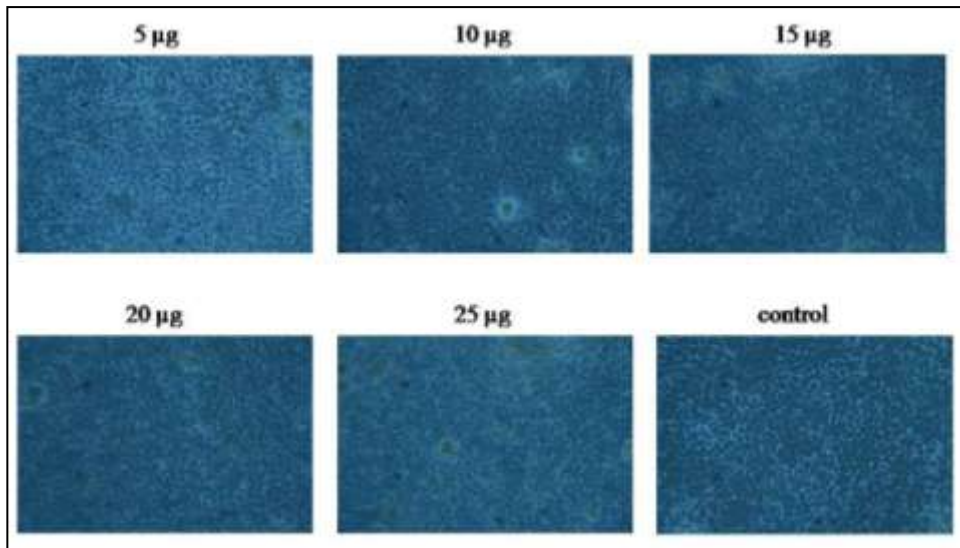


Fig-5: Antibacterial activity of the Ag Nps and Ag-PNIPAM conjugates



Enterococcus faecium

Klebsiella pneumonia



Acenitobacter baumannii

Proteus sp



Pseudomonas aeruginosa

Table-1: Antibacterial activity of the Ag Nps and Ag-PNIPAM composites

S. No	Test Organisms	Inhibitory zones (mm)	
		Ag Nps Coated	Ag-PNIPAM Coated
1	<i>Enterococcus faecium</i>	0	27.3 ± 0.56
2	<i>Staphylococcus aureus</i>	0	27.1 ± 1.03
3	<i>Klebsiella pneumoniae</i>	0	27.8 ± 0.27
4	<i>Acenitobacter baumannii</i>	0	27.3 ± 0.56
5	<i>Proteus sp</i>	0	27.6 ± 1.03
6	<i>Pseudomonas aeruginosa</i>	0	27.9 ± 0.27

Table-2: Cytotoxicity analysis of wound dressings

S. No.	Fibroblast cell lines – MTT Assay			Cytotoxic reactivity
	Concentration (µg)	Cytotoxicity (%)	Cell viability (%)	
1	5	14.7	85.3	Slight
2	10	7.1	92.9	Slight
3	15	6.5	93.5	Slight
4	20	5.2	94.8	Slight
5	25	0	>99	No cytotoxicity

References

1. Wu, T.; Ge, Z. S.; Liu, S. Y. Fabrication of Thermoresponsive Cross-Linked Poly(N-Isopropylacrylamide) Nanocapsules and Silver Nanoparticle-Embedded Hybrid Capsules with Controlled Shell Thickness. *Chem. Mater.* 2011, 23, 2370–2380.
2. Chiu, C. S.; Chen, H. Y.; Hsiao, C. F.; Lin, M. H.; Gwo, S. Ultrasensitive Surface Acoustic Wave Detection of Collective Plasmonic Heating by Close-Packed Colloidal Gold Nanoparticles Arrays. *J. Phys. Chem. C* 2013, 117, 2442–2448.
3. Tian, L. M.; Chen, E.; Gandra, N.; Abbas, A.; Singamaneni, S. Gold Nanorods as Plasmonic Nanotransducers: Distance-Dependent Refractive Index Sensitivity. *Langmuir* 2012, 28, 17435–17442.
4. Choi, J. J.; Luria, J.; Hyun, B. R.; Bartnik, A. C.; Sun, L.; Lim, Y. F.; Marohn, J. A.; Wise, F. W.; Hanrath, T. Photogenerated Exciton Dissociation in Highly Coupled Lead Salt Nanocrystal Assemblies. *Nano Lett.* 2010, 10, 1805–1811.
5. Chen, C. F.; Tzeng, S. D.; Chen, H. Y.; Lin, K. J.; Gwo, S. Tunable Plasmonic Response from Alkanethiolate-Stabilized Gold Nanoparticle Superlattices: Evidence of Near-Field Coupling. *J. Am. Chem. Soc.* 2008, 130, 824–826.
6. Li, D. X.; He, Q.; Yang, Y.; Mohwald, H.; Li, J. B. Two-Stage pH Response of Poly(4-Vinylpyridine) Grafted Gold Nanoparticles. *Macromolecules* 2008, 41, 7254–7256.
7. Tang, F.; Ma, N.; Wang, X. Y.; He, F.; Li, L. D. Hybrid Conjugated Polymer-Ag@PNIPAM Fluorescent Nanoparticles with Metal-Enhanced Fluorescence. *J. Mater. Chem.* 2011, 21, 16943–16948.
8. Mahesh D. Bedre, Raghunandan Deshpande, Basavaraj Salimath, Venkataraman Abbaraju. Preparation and characterization of polyaniline-co₃O₄ nanocomposites via interfacial polymerization. *Amer J Mat Sci.* 2012; 2(3): 39-43.
9. Shamel, K, Ahmad, MB, Md Zin Wan Yunus, W, Ibrahim, NA, Rahman, RA, Jokar, M, and Darroudi M. Silver/poly (lactic acid) nanocomposites: Preparation, characterization, and antibacterial activity. *Int J Nanomed.* 2010; 5(1): 573-579.
10. Thomas V, Yallapu MM, Sreedhar B and Bajpai SK. Breathing-in/breathing-out approach to preparing nanosilver-loaded hydrogels: Highly efficient antibacterial nanocomposites. *J. Appl. Polym. Sci.* 2008; 111: 934-944.
11. Mohan YM, Vimala K, Thomas V, Varaprasad K, Sreedhar B and Bajpai SK. Controlling of silver nanoparticles structure by hydrogel networks. *J. Colloid Interface Sci.* 2010; 342(1): 73-82.
12. Kim JS, Antibacterial activity of Ag ion-containing silver nanoparticles prepared using the alcohol reduction method. *J. Ind. Eng. Chem.* 2007; 13(5): 718-72.
13. Dror-Ehre A, H. Mamane, T. Belenkova, G. Markovich and A. Adin, J. Silver nanoparticle – *Escherichia coli* colloidal interaction in water and effect on E. coli survival. *Colloid Interface Sci.* 2009; 339: 521.
14. Saxena S and Bajpai SK, Is a Cationic-Resin-Loaded Polymeric Gel a Better Antibacterial Material than a Nanosilver-Loaded Gel. *Designed Monomers Polymers.* 2010; 13: 157-165.

15. P. Sanpui, A. Murugadoss, P. V. Durga-Prasad, S. S. Ghosh and A. Chatopadhyay, The antibacterial properties of a novel chitosan-Ag-nanoparticle composite. *Int. J. Food Microbiol.* 2008; 124: 142-146.
16. Sukumaran Prabhu and Eldho K Poulouse. Silver nanoparticles: mechanism of antimicrobial action, synthesis, medical applications, and toxicity effects. *Int Nano Lett.* 2012; 32.
17. Yun'an Qing, Lin Cheng, Ruiyan Li, Guancong Liu, Yanbo Zhang, Xiongfeng Tang, Jincheng Wang, He Liu, and Yanguo Qin. Potential antibacterial mechanism of silver nanoparticles and the optimization of orthopedic implants by advanced modification technologies. *Int J Nanomedicine.* 2018; 13: 3311–3327.